

Accepted Manuscript

Micro-Photoacoustic InfraRed Spectroscopy

Kirk H. Michaelian, Mark D. Frogley, Chris S. Kelley, Tor Pedersen, Tim E. May, Luca Quaroni, Gianfelice Cinque

PII: S1350-4495(18)30033-1
DOI: <https://doi.org/10.1016/j.infrared.2018.07.030>
Reference: INFPHY 2644

To appear in: *Infrared Physics & Technology*

Received Date: 18 January 2018
Revised Date: 12 July 2018
Accepted Date: 23 July 2018

Please cite this article as: K.H. Michaelian, M.D. Frogley, C.S. Kelley, T. Pedersen, T.E. May, L. Quaroni, G. Cinque, Micro-Photoacoustic InfraRed Spectroscopy, *Infrared Physics & Technology* (2018), doi: <https://doi.org/10.1016/j.infrared.2018.07.030>

This is a PDF file of an unedited manuscript that has been accepted for publication. As a service to our customers we are providing this early version of the manuscript. The manuscript will undergo copyediting, typesetting, and review of the resulting proof before it is published in its final form. Please note that during the production process errors may be discovered which could affect the content, and all legal disclaimers that apply to the journal pertain.



Micro-Photoacoustic InfraRed Spectroscopy

Kirk H. Michaelian¹, Mark D. Frogley², Chris S. Kelley², Tor Pedersen³, Tim E. May³, Luca Quaroni^{3,4,5}*, Gianfelice Cinque²

¹ CanmetENERGY, Natural Resources Canada, One Oil Patch Drive, Devon, Alberta T9G 1A8, Canada

² Diamond Light Source, Harwell Campus, Chilton, Oxford OX11 0DE, United Kingdom

³ Canadian Light Source Inc., University of Saskatchewan, Saskatoon, Saskatchewan S7N 2V3, Canada

⁴ Department of Experimental Physics of Complex Systems, Institute of Nuclear Physics, Polish Academy of Sciences, Kraków, 31-342, Poland

⁵ Department of Physical Chemistry and Electrochemistry, Faculty of Chemistry, Jagiellonian University, Kraków, 30-387, Poland

* Corresponding Author: Luca Quaroni, Department of Physical Chemistry and Electrochemistry, Faculty of Chemistry, ul. Gronostajowa 2, 30-387, Kraków, Poland; email: luca.quaroni@uj.edu.pl; telephone: 0048 12 686 2520

Keywords: microPAS, FT-IR, microspectroscopy, photoacoustic spectroscopy

Abstract

This investigation establishes, for the first time, the viability of micro-photoacoustic infrared spectroscopy (microPAS). A cell that allows photoacoustic (PA) infrared spectroscopy measurements on small samples was constructed and tested in this work. The setup allows visualizing the sample and selecting specific measurement positions. It can be used with conventional Fourier-Transform infrared spectrometers and a variety of light sources, including conventional near- and mid-infrared lamps, synchrotron radiation, and laser sources. The cell was successfully used to discriminate between individual polymer beads based on differences between their PA spectra. The demonstrated spatial resolution is better than 100 μm and, in at least one case, as good as 20 μm .

1. Introduction

Photoacoustic (PA) spectroscopy has been used to characterize a wide variety of materials during the last four decades. The technique belongs to the extensive group of photothermal and thermophysical methodologies, interrogating both optical and thermal properties of matter. PA spectroscopy generally enables non-destructive, non-preparative analysis of solids and liquids; this capability may be critically important in situations where sample quantities are limited and/or traditional preparation methods must be avoided. Depth

profiling of layered or inhomogeneous materials can also be effected in favourable circumstances. These attributes have motivated the development and utilization of PA spectroscopy, at a broad range of wavelengths, for many years [1].

In the infrared (IR) region, PA spectroscopy has particularly benefitted from the availability of commercial Fourier Transform Infrared (FT-IR) spectrometers, microphone-based detectors and, more recently, cantilever acoustic detectors. PA IR studies of solids have in most cases been directed to the analysis of bulk (macro) samples, with quantities on the order of a few milligrams or more being most common [2]. Despite this fact, it is important to recognize that a microsampling accessory has been manufactured by MTEC Photoacoustics for a number of years; this device was first utilized successfully to obtain PA spectra of single beads and fibres in 1999 [3]. Its design relies on the use of gaskets to locate a sample into a pre-centred location at the focal point of a parabolic mirror. The functionality of this accessory confirms that PA detection is, in fact, sufficiently sensitive to allow collection of signals from samples about 100 μm in size. The micro-sampling PA technique does not allow for visual inspection of the sample, or mapping of extended regions by selecting a region of interest across a larger sample area. With the illuminated spot neither diffraction-limited by the focusing optics nor defined by slits, its scientific utility is moderate from an IR microspectroscopy perspective.

The present article describes initial work with a novel sample cell for micro-photoacoustic spectroscopy (microPAS). This cell, designed and constructed at the Canadian Light Source, facilitates the acquisition of PA spectra of micrometre-sized solid specimens having a two-dimensional structure. In contrast with the microsampling accessory mentioned in the previous paragraph, the microPAS cell can be used together with a standard infrared microscope/FT-IR spectrometer system. This allows good spatial resolution, making it possible to move around the sample, visually inspect it and pick measurement positions, run line or raster scans, and collect images of the locations. The cell was utilized in experiments conducted at the MIRIAM beamline B22 of the Diamond Light Source during 2016. For comparison, off-line measurements were also performed at the MIRIAM beamline B22 labs using visible and infrared lasers, while FT-IR tests employed mid- and near-infrared thermal sources as well as synchrotron radiation (SR). These to our knowledge are the first proof of principle experiments of microPAS

utilizing SR IR. They serve to demonstrate the viability of the microPAS cell and, more generally, to experimentally confirm microPAS as a novel method at IR wavelengths.

2. Experimental details

2.1 MicroPAS cell design

Figure 1 presents an in-scale drawing of the microPAS cell commissioned in this work. The cell comprises a metal block enclosing a central cavity that contains the sample. The O-rings, CaF_2 visible/IR transparent windows, and retaining rings are shown above and below the cell, while the cylindrical microphone/preamplifier assembly is oriented horizontally. Two Brüel & Kjær free-field microphones, with sensitivities of 50 mV/Pa (Model 4190 paired with a Model 2669 preamplifier) and 1.1 V/Pa (Model 4955, pre-mounted with preamplifier), respectively, were utilized. A Listen SoundConnect power supply provided the necessary polarization voltages to the microphones, and also functioned as a cascaded three-stage signal amplifier/attenuator.

2.2 Laser tests

The first tests of the microPAS cell were performed using a pulsed 635-nm diode laser (average power ~5 mW) as the radiation source. A schematic layout of this table-top experiment, which employed an Agilent 33220A Function/Waveform Generator, the microphone power supply/amplifier, a Signal Recovery 7270 DSP lock-in amplifier, and an Agilent DSO7104B digital oscilloscope, is shown in Fig. 2a. The amplifier/attenuators were set to 40 dB, 0 dB and 0 dB, respectively, yielding PA signals with a maximum value of 5 V_{RMS} . Typical voltages observed for a sample of glassy carbon (thickness 60 μm) ranged from about 0.2 to 1.2 V for pulse frequencies between 3 and 40 Hz. Black plastic and a blackened aluminium disc were also tested but yielded weaker signals, hence they are not discussed further.

Further testing of the cell utilized the optics frame described in a previous publication [4]. The equipment used in this experiment is shown diagrammatically in Fig. 2b. In the first setup, the diode laser beam was made to pass through the optical system; this arrangement produced signals roughly one-third as strong as those in the initial table-top tests. More extensive multi-wavelength infrared experiments using these optics were then carried out using a Daylight Solutions TLS-41060 6.06- μm quantum cascade laser (QCL), tuneable from 5.73 to 6.39 μm

(1565–1745 cm^{-1}). This laser was operated in continuous wave (CW) mode and modulated externally at frequencies of 10 and 20 Hz using a 50% duty-cycle mechanical chopper. PA spectra of glassy carbon and polymer beads (polystyrene (PS), $\sim 35\text{--}75\ \mu\text{m}$; acetyl polystyrene (AcPS), $\sim 90\ \mu\text{m}$) were acquired step-wise by (a) adjusting the laser to an arbitrary starting wavenumber, either 1565 or 1570 cm^{-1} ; (b) manually recording the PA signals detected with the lock-in amplifier and oscilloscope; (c) incrementing the laser wavenumber setting by 5 or 10 cm^{-1} ; and (d) repeating steps (b) and (c). These large sampling intervals yielded spectra with poorer band definition than that in conventional PA FT-IR spectra of the same materials, where typical abscissa spacing is about 2 cm^{-1} .

2.3 FT-IR and microPAS

The Bruker Vertex 80v FT-IR spectrometer at the MIRIAM beamline B22 of Diamond was utilized for several experiments with the microPAS cell. The spectrometer was operated in continuous-scan mode (scanner modulation ranging from 200 Hz to 5 kHz with respect to the 15,797 cm^{-1} FT-IR sampling laser) or, alternatively, with the FT-IR scanner held in a fixed position; in the latter case a mechanical chopper provided the modulation necessary for generation of a PA signal. Thermal sources (globar and near-infrared lamps) and SR were alternately employed for the FT-IR measurements. In a preliminary test the microPAS cell was oriented vertically in the FT-IR sample compartment facing the infrared radiation emerging from the interferometer, and situated near the beam focus. The diameter of the focused SR beam in this arrangement was estimated around 1 mm FWHM.

Two additional microPAS experiments with the FT-IR spectrometer at the beamline were performed, using an ad hoc horizontal microscope and the Hyperion 3000 microscope. In the first case, horizontally directed incident radiation by-passing the Hyperion microscope was focused through a 15 \times magnification objective (numerical aperture (NA) of 0.65) mounted on an XYZ positioner. The microPAS cell was mounted vertically on a second positioner and arranged to intercept the beam (Fig. 2c). The sample, consisting of PS and AcPS beads affixed to a BaF_2 window, was visualized in transmission using a portable digital microscope situated behind the cell. This layout made it possible to locate individual beads and thus record their micro-photoacoustic spectra.

A sample section of 50 μm thick graphene oxide paper, embedded in epoxy, and characterized in detail in an earlier study [5], was also examined using the cell in the Hyperion microscope. A line spectral map was acquired and spatial resolution was evaluated by placing the microPAS cell face-down on the microscope stage, allowing SR IR to impinge on the cell from below (Fig. 2d) via a 20 \times , NA 0.5 objective. The sample was observed in transmission using visible light in order to centre it on the slits. The FT-IR scanner frequency was 200 Hz for both microscope experiments.

The properties of the light sources used in these experiments are reported in Table I, with particular reference to power and spot size.

Table 1. List of light sources used in this work and their most relevant parameters.

LIGHT SOURCE	SPECTRAL RANGE	AVERAGE POWER	SPOT SIZE (FWHM)
DIODE LASER	0.635 μm	<5 mW	~ 1 mm
QCL	5.73 - 6.39 μm	10 – 30 mW	\sim ^b
GLOBAR LAMP	1.5 - 25 μm ^a	210 W ^a	~ 1 mm
HALOGEN LAMP	1 - 5 μm ^a	750 W ^a	~ 1 mm
SYNCHROTRON RADIATION	1 - 25 μm ^{a,c}	480 W ^a	\sim ^b

^a At sample position with the FTIR optics described in the text.

^b Diffraction limited.

^c Cut-off of the beamsplitter.

3. Results and Discussion

3.1 Diode laser experiments

Signal intensities observed with glassy carbon in the microPAS cell are plotted as a function of visible diode laser pulse frequency in Fig. 3. Results for the table-top setup (Fig. 2a) are shown in Fig. 3a, while the data obtained with the optics frame are shown in Fig. 3b. The slopes of the fitted lines in these two panels are -0.88 and -0.71 , respectively; these values are somewhat less than -1.0 , which is predicted by one-dimensional Rosencwaig-Gersho theory for an optically opaque, thermally thin material [1, 2]. In idealized conditions, PA intensities of such

materials exhibit a $1/f$ dependence, but do not vary with the absorption coefficient of the material. These results demonstrate that the cell is measuring an actual PA signal.

3.2 QCL experiments

To test the capability of the cell to operate with a micrometric beam size we used the beam from a QCL laser focused inside the microPAS cell using an Agilent $15\times$ (0.6 NA) objective (Fig. 2b). With these optics in use the beam is effectively focused to a diffraction limited spot, corresponding to approximately $6\text{ }\mu\text{m}$ at the laser wavelengths in use. The QCL, also integrated with the optics frame, made it possible to acquire microPAS data from 1565 to 1745 cm^{-1} . Consistent with the comment in the preceding section, glassy carbon yielded the strongest signal, producing a broad, featureless spectral curve across this region with maximal intensity where the laser power was greatest ($\sim 1650\text{ cm}^{-1}$). This spectrum (not shown), effectively an energy curve, was used as a reference (background) to correct the AcPS and PS spectra obtained under like conditions for the response of the system optics and electronics as a function of wavelength. In these calculations, the single channel spectra acquired for AcPS and PS beads were divided by the glassy carbon spectrum, yielding the corrected spectra (discrete points connected by solid lines) in Figs. 4a and 4b. The dashed lines in both panels in this figure represent FT-IR PA spectra of bulk AcPS and PS samples previously acquired in a different laboratory in unrelated experiments [6]. Despite the coarse spacing of the QCL PA spectra, the existence of the prominent carbonyl band near 1682 cm^{-1} in Fig. 4a, attributed to the acetyl functional group in AcPS, confirms identification of these beads. This band is absent in Fig. 4b, as is expected for PS material. To summarize, the QCL experiments constitute the first successful demonstration of the capability of the microPAS cell for the analysis of micrometric samples.

3.3 FT-IR experiments

3.3.1 MicroPAS cell in FTIR sample compartment

FT-IR spectrometers have been highly successful in the measurement of broadband IR absorption spectra, including PA spectra, with high signal-to-noise ratios for several decades. It is therefore of great interest to test the performance of the microPAS cell with an FT-IR instrument, using both macroscopic and microscopic light spots, and various light sources. Initial

tests were carried out with the microPAS cell located inside the standard sample compartment of the FT-IR spectrometer. Continuous scan (200 Hz) PA spectra were acquired for a mixture of glassy carbon, PS and AcPS beads, and for these materials taken individually. Because FT-IR modulation frequency increases linearly with wavenumber, while thermal diffusion length is proportional to the inverse square root of this frequency, spatial resolution was higher (the length was smaller) at high wavenumbers. Incident radiation was derived from the internal globar and near-infrared sources, and from SR. The thermal sources yielded viable spectra by illuminating a several-millimetre diameter spot, whereas the intensities produced from SR were about an order of magnitude weaker since there is less total power in the SR beam, even though it is brighter over a ~ 1 mm diameter spot. The 1682 cm^{-1} acetyl band was well defined in the AcPS spectra obtained with the globar, as were many other features. The PS spectra lacked this band, similar to the result in section 3.2.

The beam impinging on the microPAS cell was below 1 mm in diameter when SR was utilized, and much larger for the thermal sources; hence it was inevitable that significant numbers of beads contributed to the PA intensities for this mixed sample. Like the diode laser tests described in section 3.1, this experiment confirmed the functionality of the microPAS cell, although it did not demonstrate the important capability for the analysis of individual particles or narrow spatial regions.

Another experiment was performed with glassy carbon as the only material in the cell. This test differed from the continuous-scan measurements in an essential way: the scanner in the interferometer was stopped and the incident radiation, from the globar or SR, was chopped at frequencies ranging from about 10 to 150 Hz. PA intensities observed in this experiment are plotted against chopping frequency in Figure 5. The slopes of the fitted lines in Figs. 5a and 5b, -1.07 and -1.08 for globar radiation and SR respectively, are closer to the theoretical value of -1.0 than their counterparts in Fig. 3.

3.3.2 MicroPAS via IR microbeam

Microspectroscopy experiments were next carried out with the FT-IR spectrometer system at the MIRIAM beamline B22. In this setup, depicted in Fig. 2c, the collimated beam

exited the spectrometer from the same port used for the Hyperion microscope, and bypassed the optical path leading to the microscope stage. This beam was then focused on the sample using an infinity-corrected Agilent Schwarzschild objective (15 \times ; 0.65 NA). This setup provided a focused light spot inside the microPAS cell, while avoiding the loss in throughput arising from the path through the Hyperion microscope. The same arrangement was used to focus the synchrotron beam, as well as the globar and halogen lamps in the spectrometer, in the same spot without any need for realignment. Therefore, it allowed a direct comparison of the three sources with minimal changes in the optical path within the spectrometer. The synchrotron beam was accurately collimated at the entrance pupil of the objective and provided a diffraction limited light spot at the sample. In contrast, neither the globar nor the halogen lamp delivered a collimated beam at the pupil without major loss of power; the corresponding light spots were much larger, estimated to be approximately one millimetre in size.

The objective was aligned initially with the globar and SR beams, utilizing a DTGS room temperature detector in place of the microPAS cell. Fine alignment of the optics was accomplished after this detector was replaced with the cell by chopping the beam at 10 Hz and demodulating the integrated signal with the lock-in amplifier. The chopper and lock-in were not used during measurement of the continuous-scan PA spectra. As mentioned in section 2.3 and shown in Fig. 2c, the cell was oriented vertically during these experiments.

Preliminary measurements were made on PS and AcPS samples, employing visual inspection to ensure that the focused beam was directed onto the beads: the microPAS cell position was finely adjusted to maximize PA intensities. Spectra were acquired for both types of beads using the FT-IR internal mid- and near-infrared sources, as well as SR. Better results were obtained with SR IR for both materials. For example, Fig. 6a compares PS spectra acquired with SR and the two thermal sources: SR yielded a viable spectrum (red curve); while the spectra obtained with the internal sources (blue and green traces) were of lower quality (signal/noise ratios ~ 2). The identification of PS and AcPS is easily made through a comparison of different SR spectra (Fig. 6b).

Single bead measurements were then performed with the same optical setup. A portable digital microscope situated behind the microPAS cell allowed observation of the visible component of the incident light accompanying the IR radiation. The beam from the He-Ne laser

in the spectrometer was coincident with the IR beam for all sources, enhancing visualization and alignment of individual beads. Several beads were selected for analysis in this way. MicroPAS spectra of these beads were recorded using SR as the source. Identification of particular beads as PS or AcPS, based on similarities with the spectra acquired earlier in this study, was straightforward.

Two examples serve to illustrate the capability of the microPAS cell for the analysis of single beads. Fig. 7 shows two of the best spectral quality data acquired from an arbitrarily selected bead (illuminated) in the photograph. Measurement of this spectrum, at a scan rate of 200 Hz, required 38 min. In the second example a different spectrum was obtained for another bead (Fig. 8) in the same acquisition conditions, with the absence of the acetyl band confirming the identity of the second bead as PS. Thus the two bead types were readily identified as AcPS or PS from their micro-photoacoustic spectra, based on the characteristic acetyl band at 1682 cm^{-1} ; similar results were obtained even by co-adding 16 scans, which required less than 5 min acquisition time. Recalling the dimensions of the beads given earlier, these results are consistent with the statement that the spatial resolution of the combined microscope/microPAS cell setup is better than the $\sim 100\text{ }\mu\text{m}$ bead size.

3.3.3 Linescan microPAS and SR-IR spatial resolution

In a final test, we positioned the microPAS cell on the stage of the Hyperion microscope, using the normal optical path for IR spectromicroscopy experiments (Fig 2d). The standard Bruker $15\times$ (Newport, 0.40 NA) microscope objective was used to focus the beam. This configuration produces a major loss in throughput. As a consequence, the diffraction-limited SR beam in the sample plane has a power of approximately $90\text{ }\mu\text{W}$. However, this configuration also allows use of the automated motor-controlled stage to perform 1D and 2D mapping experiments.

A sample of graphene oxide (GO) paper embedded in epoxy was used to demonstrate the capability of the microPAS cell for use in a line spectral map, and to obtain a better estimate of spatial resolution. These measurements utilized the fact that GO produces nearly featureless micro-photoacoustic spectra, like those from glassy carbon. By contrast, the epoxy substrate yields a weaker spectrum containing bands due to several functional groups.

Figure 9 displays an image of the GO/epoxy sample in addition to several spectra. In this experiment, the position of the cell was shifted by successive increments (25 μm steps in the proximity of the GO layer and 50 μm steps elsewhere) in the direction perpendicular to the GO stripe. The upper curve in the middle panel is the spectrum recorded at the location where the GO contribution was greatest. Epoxy bands near 1170, 1250, 1600, 1730 and $\sim 2900\text{ cm}^{-1}$ contribute slightly to this spectrum, which was generally not expected to contain any well-defined bands. Negative-going bands due to ambient water vapour ($\sim 1600\text{--}1700\text{ cm}^{-1}$) and CO_2 ($\sim 2350\text{ cm}^{-1}$) further affect the results, as does absorption due to the diamond window (negative features around $2000\text{--}2300\text{ cm}^{-1}$). The lower curve represents an epoxy spectrum obtained for a spot far from the GO.

A three-dimensional display of the entire series of spectra recorded in this experiment appears in the bottom panel of Fig. 9. Microscope stage positions, relative to an arbitrary zero, are reported in micrometres. The foreground spectrum is attributed to epoxy alone. As the position shifts along the z -axis, approaching $2550\text{ }\mu\text{m}$, the PA spectra gradually take on the broad featureless shape expected for GO. Further movement of the stage shifted the sample such that the contribution from epoxy again dominates. The total translation distance was about $400\text{ }\mu\text{m}$.

Spatial resolution was determined using a modified experimental configuration. Metal slits in the incident beampath defined a maximum spot size at the sample of $40\text{ }\mu\text{m}$. Integrated PA intensity was measured by stopping the FT-IR scanner, chopping the beam, and demodulating the signal with the lock-in amplifier. Because the GO absorption was stronger than that of epoxy, the integrated signal became significantly greater when the SR beam impinged on GO. Results from this test are plotted in Fig. 10. The width of the profile is significantly less than $100\text{ }\mu\text{m}$, and, given the $\sim 50\text{ }\mu\text{m}$ width of the GO paper (Fig. 9), the actual spatial resolution is likely below the $40\text{ }\mu\text{m}$ slit size and closer to the diffraction limit since the SR beam is brightest at the slit centre. The spatial resolution of the microscope/microPAS system in this setup is estimated to be approximately $20\text{ }\mu\text{m}$ FWHM.

4. Conclusions

This article describes the proof of principle of microPAS using synchrotron based FT-IR and the commissioning of a novel sample accessory for infrared micro-photoacoustic

spectroscopy. A purpose-built microPAS cell allowed focusing of the light beam onto the sample and the recording of PA spectra from micrometric structures. Off-line tests were performed using laser sources. FT-IR measurements were also performed using thermal sources and synchrotron radiation. The cell, which is compatible with a standard FT-IR microscope/spectrometer system, was installed and tested on the Hyperion microscope at the MIRIAM beamline B22 of the Diamond Light Source. The use of bright synchrotron radiation allowed measurements with diffraction limited light spots, with sizes comparable to the radiation wavelength. Viable mid-infrared spectra were obtained for single polymer beads with dimensions between 35 and 90 μm . A line spectral map for a graphene oxide/epoxy sample confirmed that the spatial resolution of the microPAS accessory is better than 100 μm and as good as 20 μm in some circumstances. The microPAS capability will be further explored and tested more extensively in future experiments at Diamond using research microsamples where standard FT-IR microspectroscopy is incapable of providing results.

Acknowledgments: We thank Congwei Wang (CAS Key Laboratory of Carbon Materials, Institute of Coal Chemistry, Taiyuan, P.R. China) for preparation of the GO sample. This work was carried out with the support of the Diamond Light Source (proposal SM13668-1) and of the Canadian Light Source. The Canadian Light Source is supported by the Canada Foundation for Innovation, Natural Sciences and Engineering Research Council of Canada, the University of Saskatchewan, the Government of Saskatchewan, the National Research Council Canada, Western Economic Diversification Canada, and the Canadian Institutes of Health Research. This project has received funding by the European Union's Horizon 2020 research and innovation programme under the Marie Skłodowska-Curie grant agreement No. 665778 (POLONEZ 2 fellowship to Luca Quaroni, managed by the National Science Center Poland under contract UMO - 2016/21/P/ST4/01321).

Declarations of interest: none

References

1. A. Rosencwaig. Photoacoustics and Photoacoustic Spectroscopy. Wiley-Interscience, New York, 1980.
2. K.H. Michaelian. Photoacoustic IR Spectroscopy. Instrumentation, Applications and Data Analysis, 2nd ed. Wiley-VCH, Weinheim, 2010.

3. E.Y. Jiang. *Appl. Spectrosc.* 53, 583 (1999).
4. P.M. Donaldson, C.S. Kelley, M.D. Frogley, J. Filik, K. Wehbe, G. Cinque. *Opt. Express* 24, 25219 (2016).
5. M.D. Frogley, C. Wang, G. Cinque, A.H. Barber. *Vib. Spectrosc.* 75, 178 (2014).
6. Q. Wen, K.H. Michaelian. *Spectrochim. Acta A* 73, 823 (2009).

Captions to Figures

Fig. 1 Micro-photoacoustic cell constructed at the Canadian Light Source. The optical windows, retaining rings and O-rings are shown above and below the cell body, which was machined from brass. The cylindrical microphone is situated on the right-hand side.

Fig. 2 Apparatus for microPAS cell tests with (a) diode laser side view; (b) diode laser or QCL in optics frame side view; (c) microscope/FT-IR system, microscope side port top view; (d) microscope/FT-IR system, side view.

Fig. 3 Variation of microPAS signal with laser pulse frequency for 60- μm glassy carbon. (a) offline (table-top) experiment; (b) laser installed in optics frame. The slopes of the fitted lines are -0.88 and -0.70 in (a) and (b), respectively.

Fig. 4 Comparison of microPAS spectra obtained using QCL excitation (solid lines) with conventional (macro) FT-IR PA spectra (dashed lines). (a) acetyl polystyrene; (b) polystyrene. FT-IR spectra were rescaled and shifted vertically to facilitate comparison where necessary.

Fig. 5 Variation of microPAS signal with chopping frequency for 60- μm glassy carbon. The cell was oriented vertically in the FT-IR sample compartment, and the scanner (moving mirror) was stationary during data acquisition. Radiation sources were (a) globar; (b) SR. The slopes of the fitted lines are -1.07 and -1.08 in (a) and (b), respectively.

Fig. 6 (a) MicroPAS spectra (64 scans, 16 cm^{-1} resolution) of polystyrene acquired with the Schwarzschild objective and the configuration in Fig. 2c. Radiation sources were SR (red

curve); mid-IR (blue); near-IR (green). (b) Spectra (128 scans, 16 cm^{-1}) for acetyl polystyrene (blue) and polystyrene (red) obtained using SR.

Fig. 7 (top panel) Spectrum of a single bead acquired with the microPAS cell and the Hyperion microscope/FT-IR system (Average of two spectra; resolution, 16 cm^{-1} ; 64 scans; 200 Hz). Identification of the bead as AcPS is confirmed by the acetyl band at 1682 cm^{-1} . (bottom panel) Photograph of sample consisting of AcPS and PS beads. The brightly illuminated bead in the lower left quadrant was analyzed in this experiment.

Fig. 8 (top panel) PA spectrum of another single bead, acquired under conditions similar to those in Fig. 6. The bead is identified as PS from the absence of the acetyl band at 1682 cm^{-1} . (bottom panel) Photograph of sample showing the bead (illuminated) giving rise to this spectrum. The field of view is the same as in Fig. 6.

Fig. 9 (top panel) Optical image of GO paper ($50\text{ }\mu\text{m}$ thickness) within the epoxy sample; (middle panel) PA spectra of GO and epoxy acquired with SR; (bottom panel) line spectral map obtained with $100\text{ }\mu\text{m}$ slit width. Greatest GO intensity exists near the $2550\text{ }\mu\text{m}$ position on the z -axis.

Fig. 10 Spatial resolution test for GO paper/epoxy sample ($40\text{ }\mu\text{m}$ slit width). The profile was measured using $10\text{ }\mu\text{m}$ steps. The peak in the integrated signal is due to GO. Abscissa units are the same as those for the z -axis in Fig. 8, bottom panel.

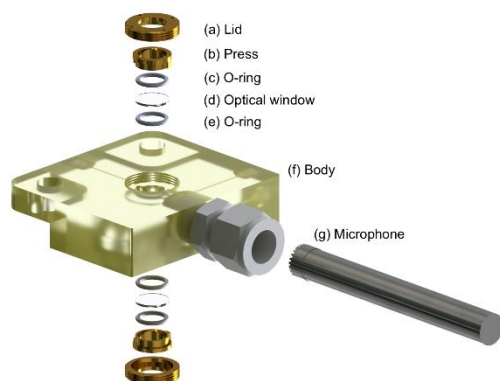


Fig. 1

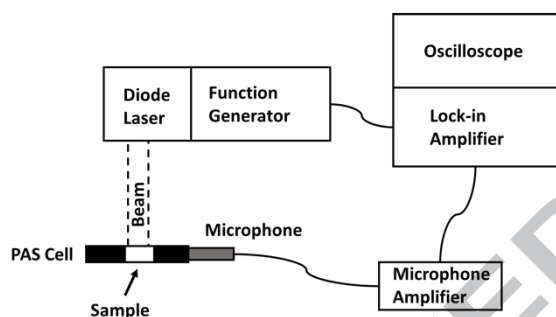


Fig. 2a

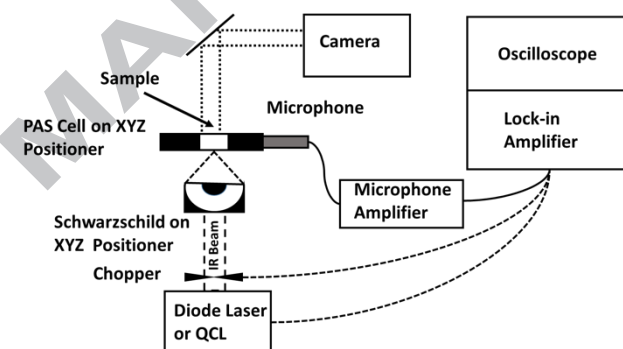


Fig. 2b

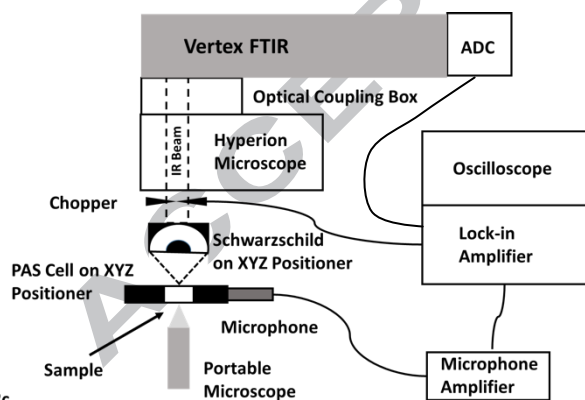


Fig. 2c

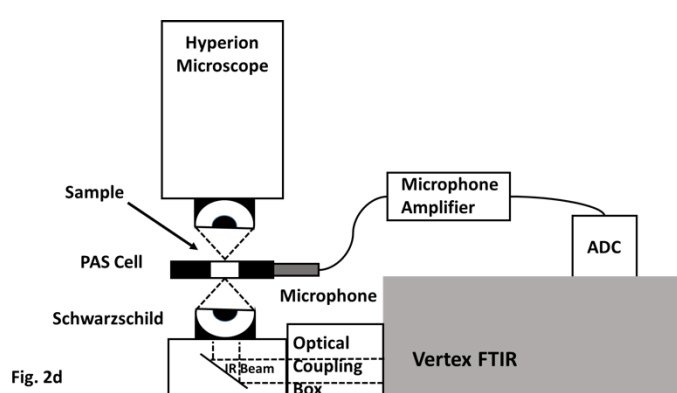


Fig. 2d

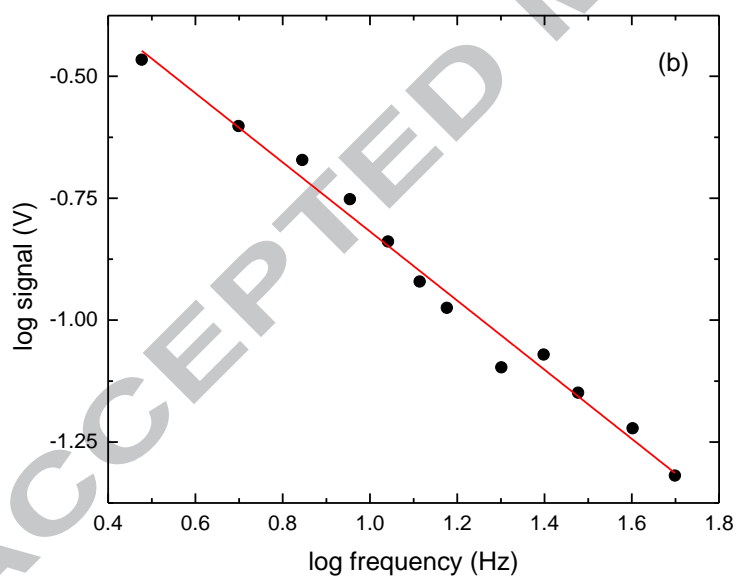
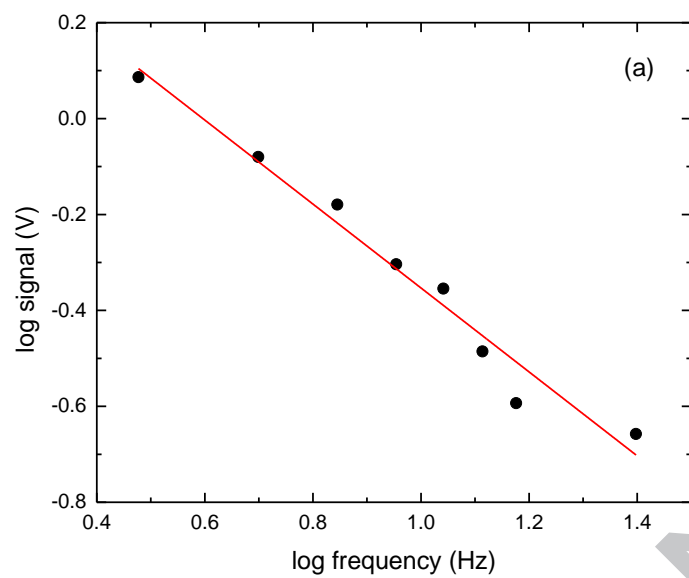


Fig. 3

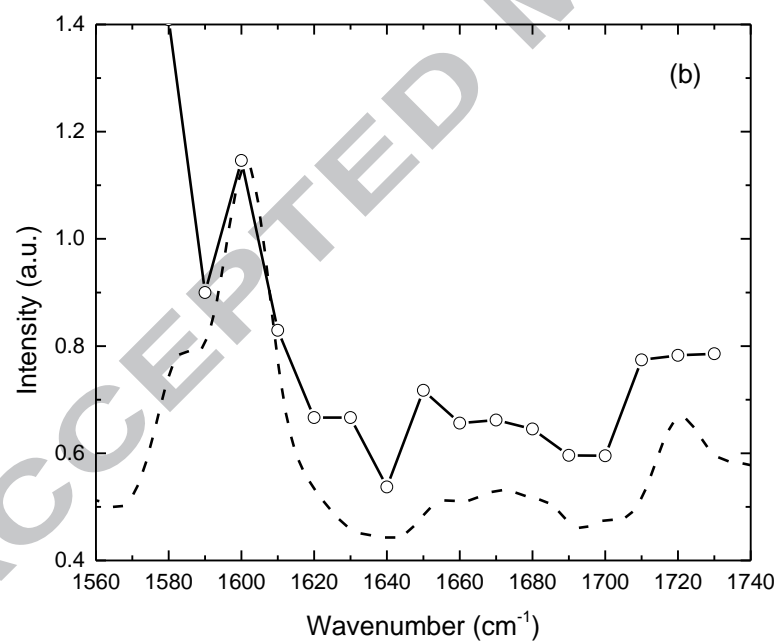
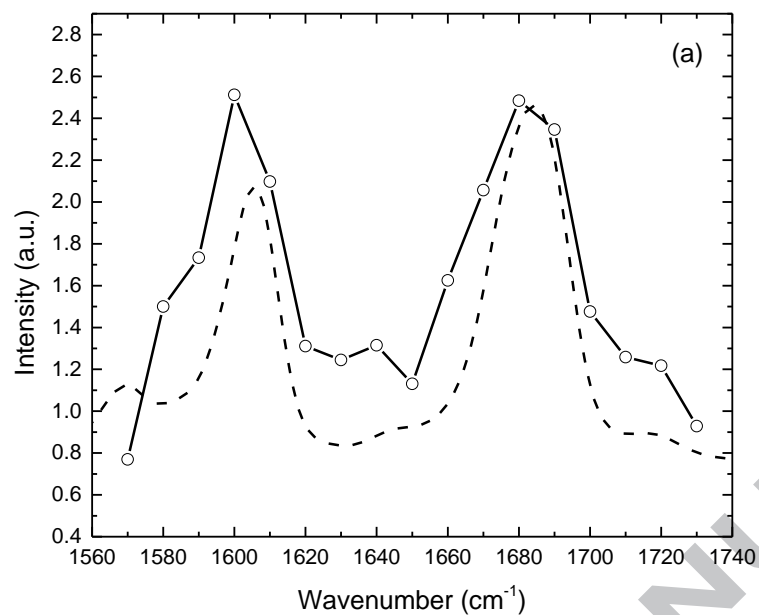


Fig. 4

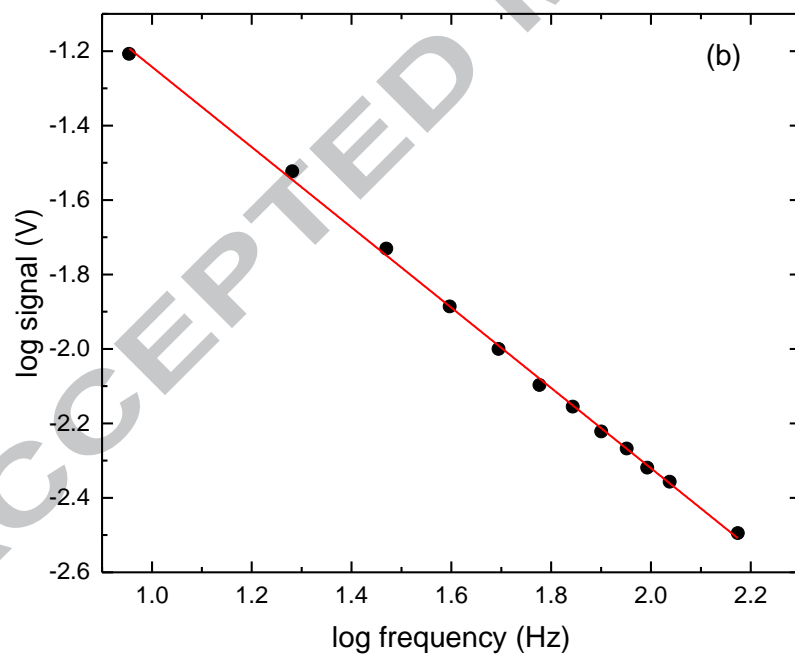
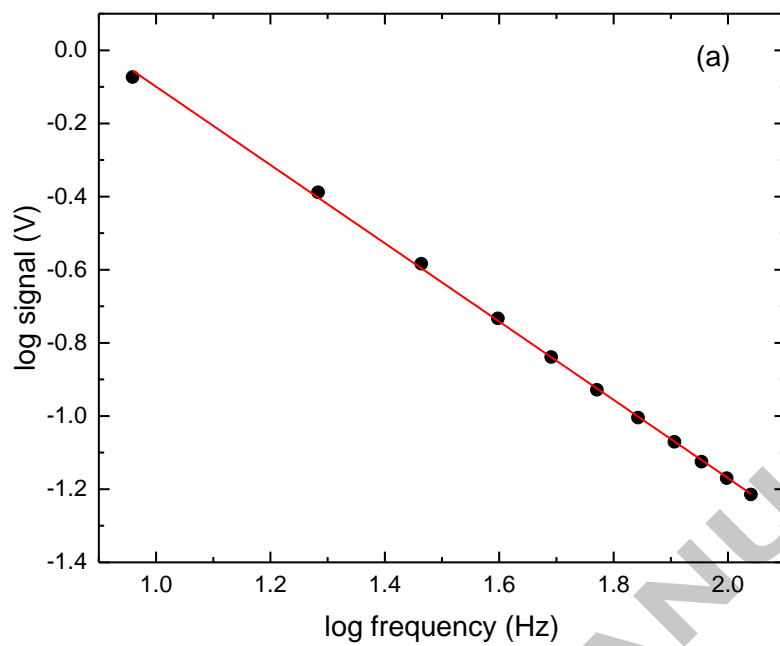


Fig. 5

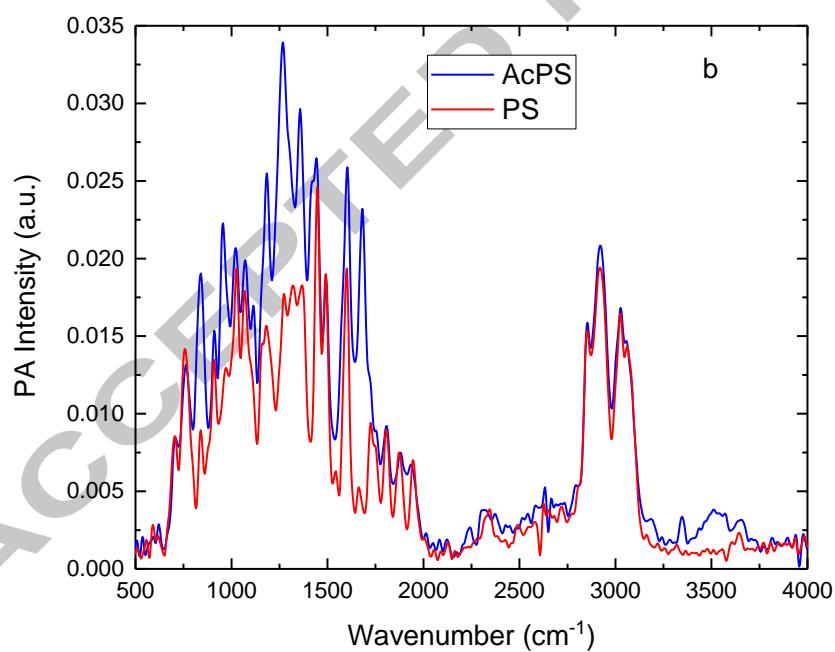
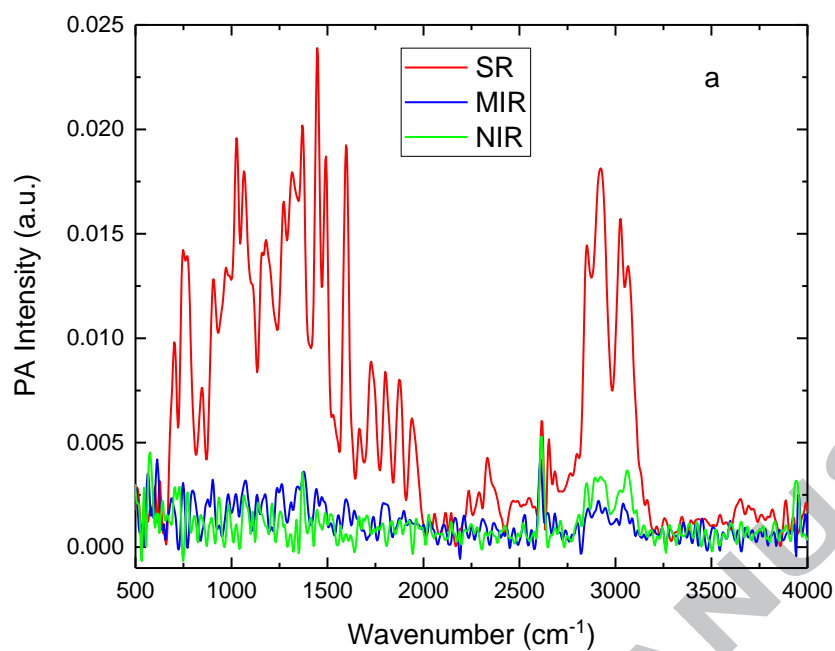


Fig. 6

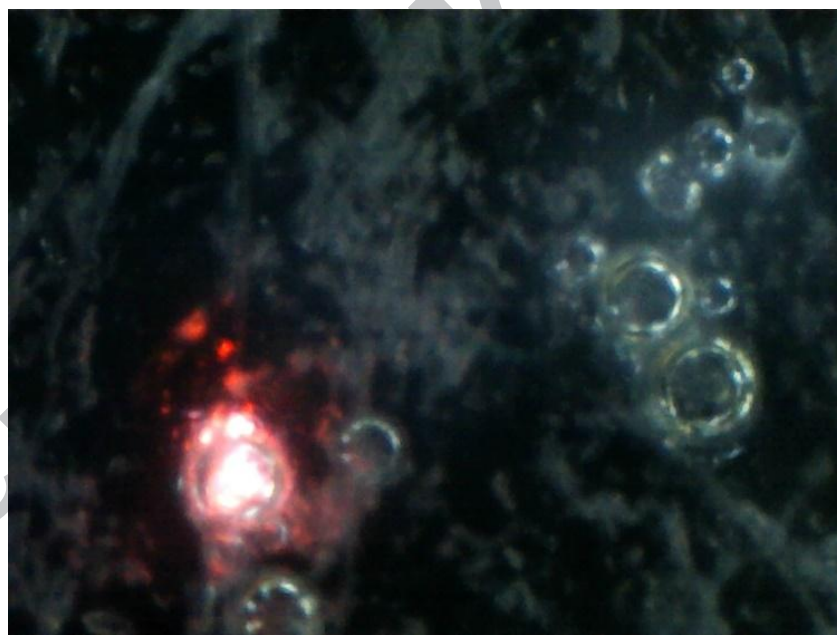
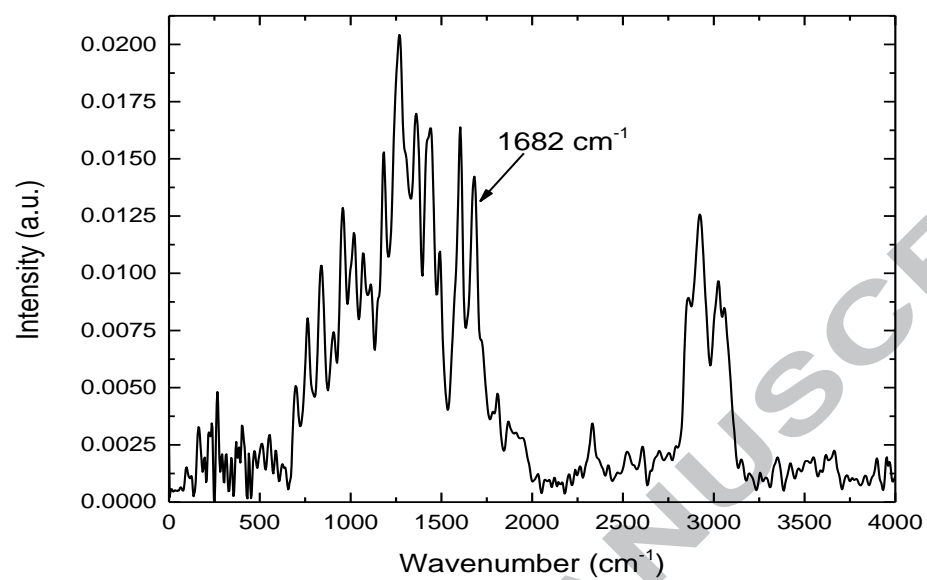


Fig. 7

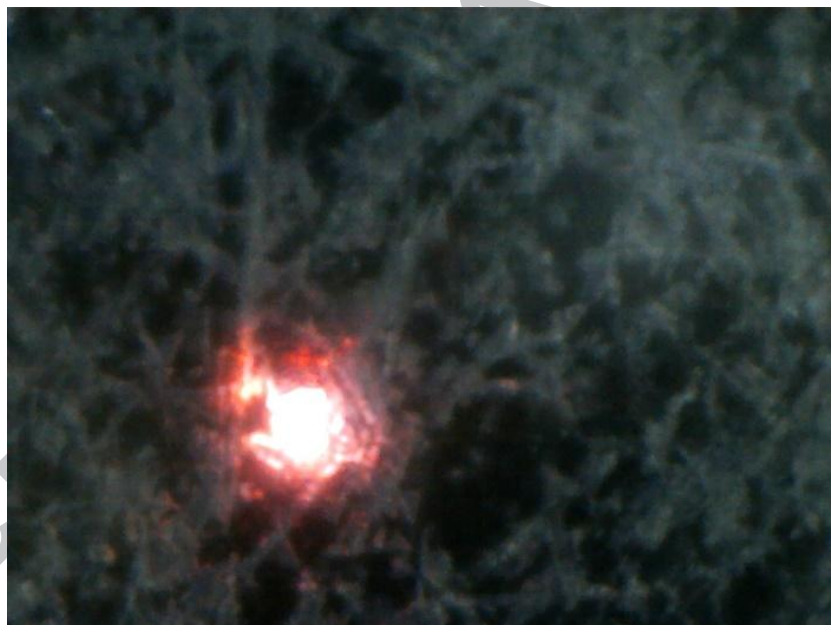
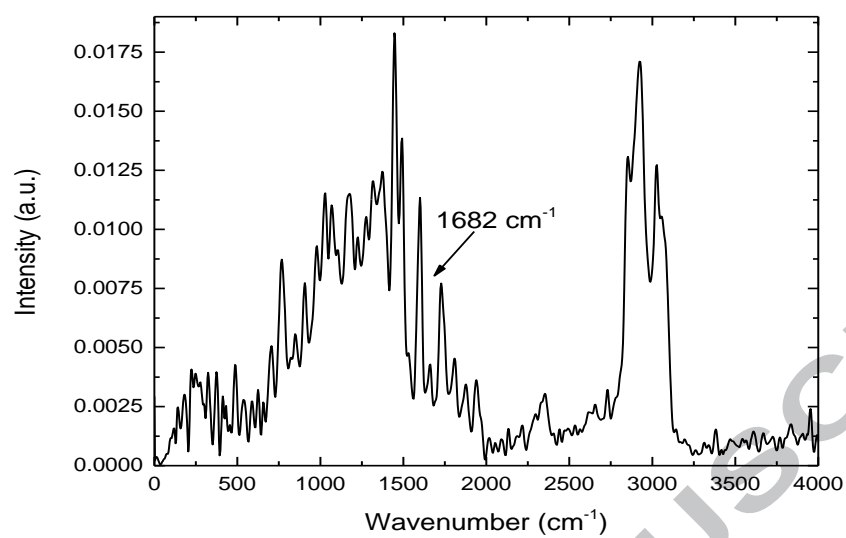


Fig. 8

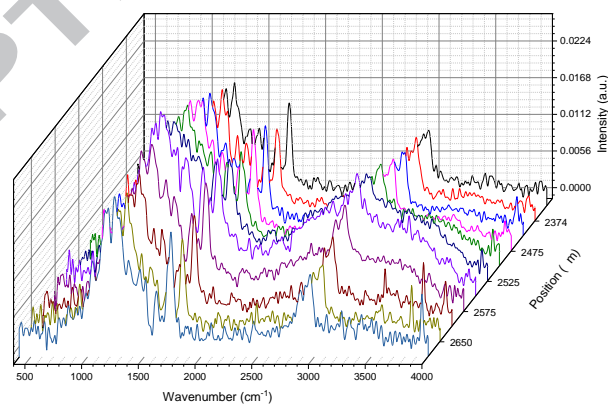
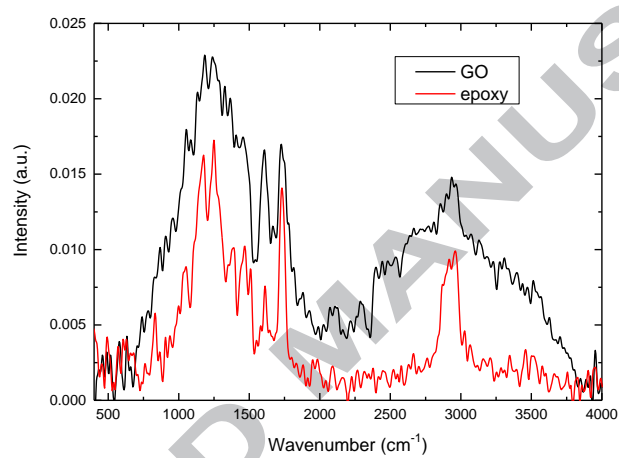
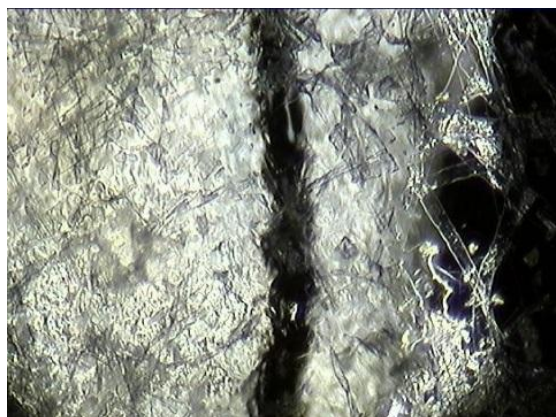


Fig. 9

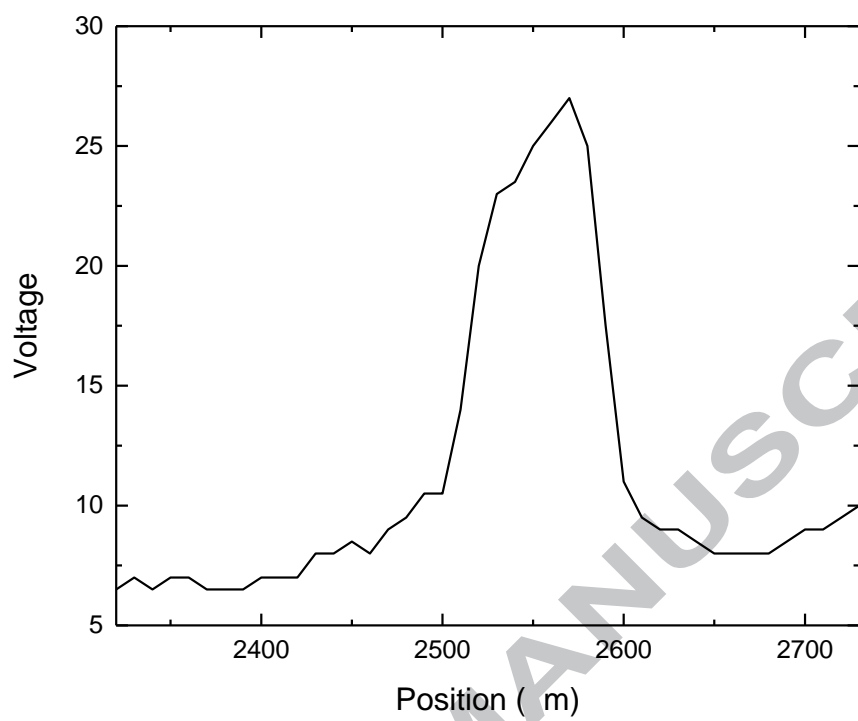


Fig. 10

Declarations of interest: none

ACCEPTED MANUSCRIPT

Highlights

We introduce mid-infrared photoacoustic spectroscopy in a microscopy configuration (microPAS)

We describe a cell that allows single-point and mapping microPAS measurements.

We show that by using synchrotron radiation we can perform mid-infrared FTIR microPAS measurements with a diffraction-limited light spot.